

This is a self-archived version of an original article. This version may differ from the original in pagination and typographic details.

Author(s): Tahkola, Kyösti; Ahtiainen, Maarit; Mecklin, Jukka-Pekka; Kellokumpu, Ilmo; Laukkarinen, Johanna; Tammi, Markku; Tammi, Raija; Väyrynen, Juha P.; Böhm, Jan

Title: Stromal hyaluronan accumulation is associated with low immune response and poor prognosis in pancreatic cancer

Year: 2021

Version: Published version

Copyright: © The Author(s) 2021

Rights: CC BY 4.0

Rights url: <https://creativecommons.org/licenses/by/4.0/>

Please cite the original version:

Tahkola, K., Ahtiainen, M., Mecklin, J.-P., Kellokumpu, I., Laukkarinen, J., Tammi, M., Tammi, R., Väyrynen, J. P., & Böhm, J. (2021). Stromal hyaluronan accumulation is associated with low immune response and poor prognosis in pancreatic cancer. *Scientific Reports*, 11, Article 12216. <https://doi.org/10.1038/s41598-021-91796-x>



OPEN

Stromal hyaluronan accumulation is associated with low immune response and poor prognosis in pancreatic cancer

Kyösti Tahkola^{1,2}✉, Maarit Ahtiainen³, Jukka-Pekka Mecklin^{4,5}, Ilmo Kellokumpu¹, Johanna Laukkarinen^{2,6}, Markku Tammi⁷, Raija Tammi⁷, Juha P. Väyrynen^{3,8} & Jan Böhm³

Hyaluronan (HA) accumulation has been associated with poor survival in various cancers, but the mechanisms for this phenomenon are still unclear. The aim of this study was to investigate the prognostic significance of stromal HA accumulation and its association with host immune response in pancreatic ductal adenocarcinoma (PDAC). The study material consisted of 101 radically treated patients for PDAC from a single geographical area. HA staining was evaluated using a HA-specific probe, and the patterns of CD3, CD8, CD73 and PD-L1 expression were evaluated using immunohistochemistry. HA staining intensity of tumour stromal areas was assessed digitally using QuPath. CD3- and CD8-based immune cell score (ICS) was determined. High-level stromal HA expression was significantly associated with poor disease-specific survival ($p=0.037$) and overall survival ($p=0.013$). In multivariate analysis, high-level stromal HA expression was an independent negative prognostic factor together with histopathological grade, TNM stage, CD73 positivity in tumour cells and low ICS. Moreover, high-level stromal HA expression was associated with low ICS ($p=0.017$). In conclusion, stromal HA accumulation is associated with poor survival and low immune response in PDAC.

Abbreviations

HA	Hyaluronan
ICS	Immune cell score
PDAC	Pancreatic ductal adenocarcinoma
DSS	Disease-specific survival
OS	Overall survival
TMA	Tissue microarray

Pancreatic ductal adenocarcinoma (PDAC) is one of the most aggressive solid malignancies with 5-year survival rates of 2–9%^{1,2}. This is partly related to advanced disease stage at the time of diagnosis ruling out curative surgery. Tumour cells are in constant interaction with non-neoplastic cells, and the tumour microenvironment influences cancer progression. PDAC has been shown to develop mechanisms that suppress the host immune response against the tumour³. The first signs of this immune suppression are seen already in the premalignant lesions⁴. PDAC is characterized by an abundant desmoplastic stroma, which has been suggested to facilitate the escape from the immune surveillance^{5,6}.

Hyaluronan (HA) is one of the main components of the extracellular matrix. In normal physiological conditions, it is strongly expressed during wound healing and at sites of inflammation, including cancer⁷. It also

¹Department of Surgery, Central Finland Health Care District, Jyväskylä, Finland. ²Faculty of Medicine and Health Technology, Tampere University, Tampere, Finland. ³Department of Pathology, Central Finland Health Care District, Jyväskylä, Finland. ⁴Department of Education and Research, Central Finland Health Care District, Jyväskylä, Finland. ⁵Sport&Health Sciences, University of Jyväskylä, Jyväskylä, Finland. ⁶Department of Gastroenterology and Alimentary Tract Surgery, Tampere University Hospital, Tampere, Finland. ⁷Institute of Biomedicine, School of Medicine, University of Eastern Finland, Kuopio, Finland. ⁸Cancer and Translational Medicine Research Unit, Medical Research Center Oulu, University of Oulu and Oulu University Hospital, Oulu, Finland. ✉email: kyosti.tahkola@kssh.fi

influences immune responses⁸. A complex regulation system controls HA metabolism, mainly dependent on HA-producing synthases and degrading hyaluronidases. The activation of the cell surface HA receptors such as CD44⁹ and RHAMM¹⁰ modulate cell proliferation, aggregation, migration and angiogenesis¹¹ and may also be involved in the HA-induced epithelial–mesenchymal transition¹² and stem cell functions¹³. HA has been shown to be overexpressed in most human malignancies^{14–23}. Several studies have indicated that hyaluronan accumulation in the tumour cells and/or peritumoral stroma is related to tumour progression and poor survival in many cancer types^{23–31}. However, the mechanisms underlying the association between accumulation of HA, host immune response and poor survival remain unclear, especially in PDAC.

The association between a strong immune response and better survival is well established in various cancers^{32–36}. We have previously introduced a T-lymphocyte-based immune cell score (ICS) as a strong favourable prognostic factor in PDAC³⁷. Extensive alterations occur in the complex PDAC microenvironment during the tumorigenesis. Multiple mechanisms, such as overexpression of the immunosuppressive molecules CD73 and PD-L1, may lead to immune suppression^{38–41}. There is some evidence showing that HA plays a role in immune response regulation^{42,43}. According to our hypothesis this might be one of the key factors explaining the association between HA accumulation and low survival among cancer patients²⁵.

The aim of the present study was to examine the prognostic role of stromal HA accumulation and its relation to immune cell infiltration and the immune-suppressing molecules CD73 and PD-L1 in PDAC.

Methods

Patients. From 2000 to 2016, a total of 129 patients with PDAC were operated on with curative intent in the Central Hospital of Central Finland, Jyväskylä, Finland. Patients with locally inoperable tumour, peritoneal carcinosis or distant metastases were excluded, resulting in the 101 patients with stage IA–IIB disease. Detailed information on patient and tumour characteristics, surgical treatment and complications, oncological treatment and follow-up were collected prospectively, updated and confirmed by a review of patient records review. None of the included patients received neoadjuvant chemotherapy before surgery.

Histopathological examination. All histopathological tumour specimens were reviewed by an experienced gastrointestinal histopathologist (JB). Tumour staging was done according to the 7th edition of the UICC/AJCC TNM categories⁴⁴. The grading was performed according to the WHO classification of tumours 2010⁴⁵.

Tumour sampling, HA assay, and immunohistochemistry. Tissue microarray (TMA) blocks were constructed as described previously, from formalin-fixed paraffin-embedded primary PDAC patient tumour samples. Two tissue cores 0.6 mm in diameter were taken both from the core of the tumour and the invasive margin from representative tumour blocks. Sections of 2 µm thickness were used for immunohistochemical (IHC) analyses³⁷.

Hyaluronan was stained as described previously²⁶. Briefly, a complex containing the G1 domain of cartilage aggrecan and link protein was labeled with biotin (bHABC), diluted to 3 µg/ml of 1% bovine serum albumin in phosphate buffer, and incubated overnight at 4 °C on sections pretreated with H₂O₂ and 1% bovine serum albumin to block endogenous peroxidases and unspecific binding, respectively. After one hour incubation in avidin–biotin–peroxidase (Vector Laboratories, Irvine, CA; 1:200 dilution) the sections were washed with PBS, and incubated in 0.05% 3,3'-diaminobenzidine (Sigma Chemical Co., St. Louis, MO) and 0.03% H₂O₂ in the phosphate buffer, followed by nuclear counterstaining with Mayers hematoxylin (Fig. 1). Staining for CD73 was conducted as described previously, with rabbit monoclonal anti-CD73 antibody (D7F9A, Cell Signalling) and ultraView Universal DAB detection kit (Roche) for Ventana³⁹ (Fig. 2). Staining for CD3 and CD8 was conducted with anti-CD3 (LN 10, 1:200; Novocastra) and anti-CD8 (SP16, 1:400; Thermo Scientific) antibodies, using a Lab Vision Autostainer 480 (Immunovision Technologies Inc.) (Fig. 3). Staining for PD-L1 was conducted as described previously, with anti-PD-L1 (E1L3N, 1:100; Cell Signalling Technology) antibody, using a BOND-III stainer (Leica Biosystems). PD-L1 staining was carried out using whole tissue sections³⁷ (Fig. 4).

Signal visualization for all IHC was done by diaminobenzidine and sections were counterstained with haematoxylin.

In general, HA staining was clearly seen in all specimen both in stroma and in tumour epithelium. Stained TMA sections were scanned using an Aperio digital slide scanner (Leica Biosystems), followed by analysis using QuPath v 0.1.2 as described below.

ICS was determined using the TMA technique as described earlier³⁷. Briefly, ICS describes the immune response represented by the density of CD3 and CD8 positive immune cells in the tumour centre and at the invasive margin. PD-L1 expression was evaluated by estimating the proportion of PD-L1 positivity on the tumour cell surface as described earlier³⁹. In addition, we analyzed also the proportion of PD-L1 expression in stromal cells using the 5% staining proportion as a cutoff.

Quantitative evaluation of HA staining. HA was evaluated using QuPath v 0.1.2⁴⁶. First, the stain vectors and background values were estimated using the *Estimate stain vectors* command to facilitate stain separation with the color deconvolution method. *Simple tissue detection* command was used to delineate the tissue area from the white background. This area was manually edited with the brush tool to exclude tumour epithelial regions. *SLIC superpixel segmentation* was used to divide the area into superpixels (neighboring groups of pixels sharing similar characteristics). DAB intensity was calculated for each superpixel, and the data were exported at individual superpixel level. R statistical programming language version 3.5.2 (R Foundation for Statistical Computing, Vienna, Austria) was used to summarize the mean intensity for each case. The distribution of DAB intensities was similar in different TMAs suggesting that the assay had performed uniformly (Fig. S.1). The cores

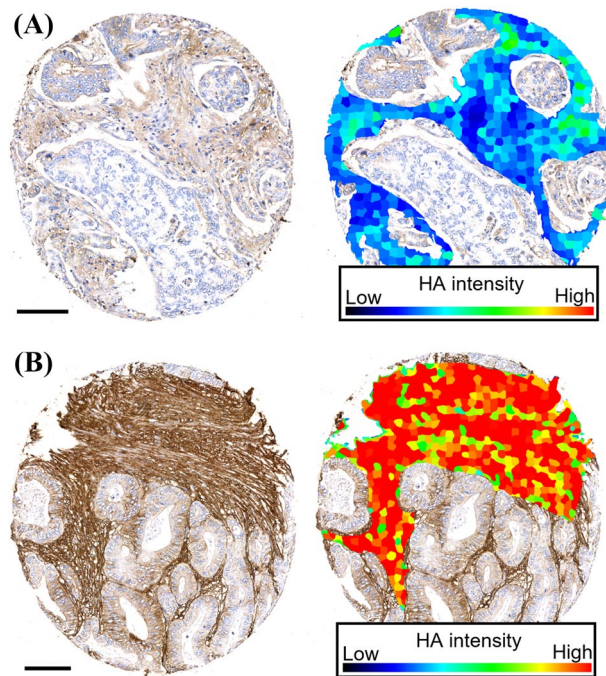


Figure 1. Representative examples of tissue microarray cores with low (A) and high (B) stromal hyaluronan (HA) intensity. The images show the exclusion of the tumour parenchyma and the delineation of the superpixels formed by the program used for analysis. Scale bars indicate 100 μ m.

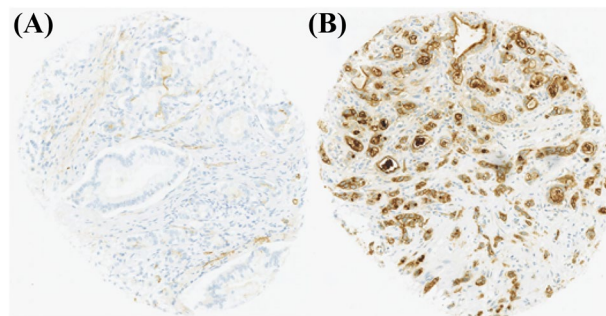


Figure 2. Representative examples of tissue microarray cores with low (A) and high (B) expression of CD73.

from tumour centre and invasive margin had a strong positive correlation (Spearman's $\rho = 0.69$), and average HA intensity of all available tumour regions was therefore used in the main analyses.

Samples were divided into two groups based on the mean intensity value: high and low stromal HA expression. To determine cut-off values for HA expression with optimal sensitivity and specificity, we used receiver operating characteristic (ROC) curve drawn in relation to disease-specific 3-year mortality.

Statistical analyses. The chi-square test was used when analysing the associations between HA and clinical and histopathological variables, CD73 positivity and PD-L1 positivity in tumour cells. The estimates for hazard ratios for overall survival (OS) and disease specific survival (DSS) were calculated using univariate and multivariate Cox proportional hazards regression model. Only variables with $p < 0.05$ in univariate analysis were entered into the multivariate analysis despite the a-priori determined confounder, tumour stage ($p = 0.117$). All statistical tests were two-sided. A p value less than 0.05 was considered significant. The statistical analyses were performed and Fig. 5 created with IBM SPSS statistics 24 for Windows (IBM Corporation, Armonk, NY, USA, <https://www.ibm.com/analytics/spss-statistics-software>).

Compliance with ethical standards. The use of patient samples and the data inquiry were approved by the Oulu University Hospital Ethics Committee. The need to obtain written or oral consent from patients to use their samples in research was waived by the Finnish National Authority for Medicolegal Affairs (VALVIRA,

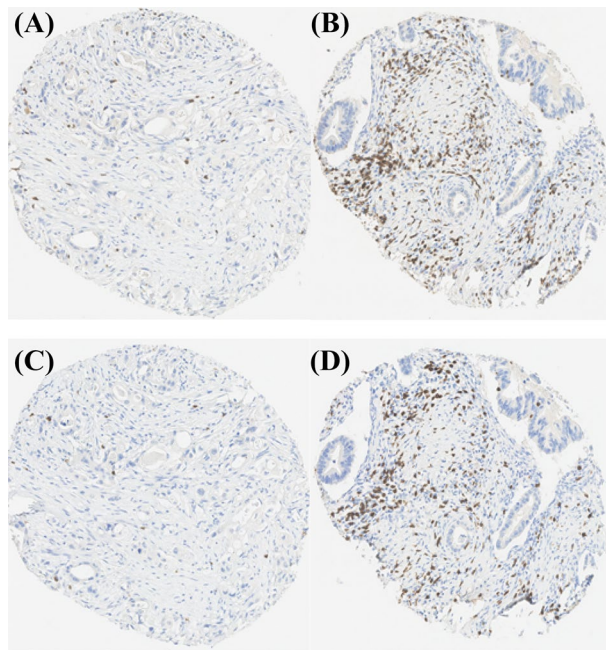


Figure 3. Representative examples of tissue microarray cores with low (A) and high CD3+ (B), and CD8+ (C,D) T-cell densities.

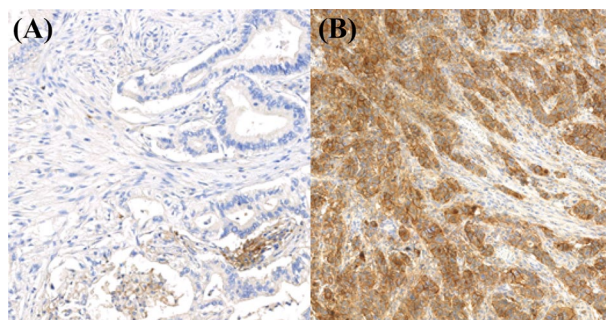


Figure 4. Representative examples of PD-L1 negative (A) and positive (B) tumour samples.

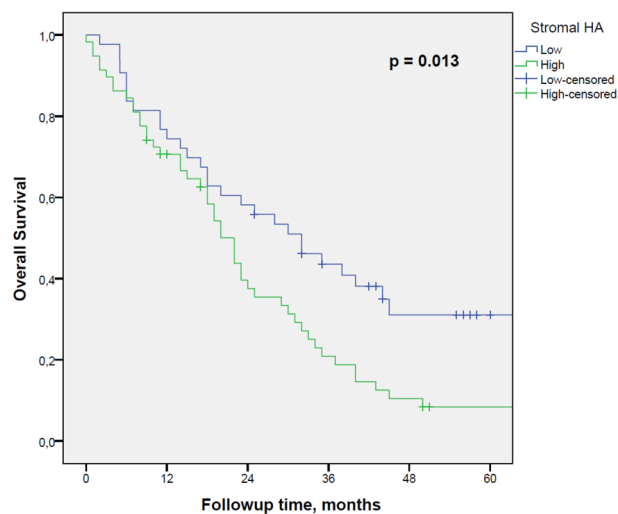


Figure 5. Prognostic impact of stromal HA content on survival on OS.

Total, n	101
Age, years	
Median	67
Range	45–82
Gender, n (%)	
Male	53 (52.5)
Female	48 (47.5)
T-stage, n (%)	
pT1	3 (3.0)
pT2	22 (21.8)
pT3	76 (75.2)
pT4	0 (0)
N-stage, n (%)	
pN0	30 (29.7)
pN1	71 (70.3)
Stage, n (%)	
IA	3 (3.0)
IB	7 (6.9)
IIA	20 (19.8)
IIB	71 (70.3)
Histological grade, n (%)	
1	29 (28.7)
2	60 (59.4)
3	7 (6.9)
Unknown	5 (5.0)
Perineural invasion, n (%)	
Positive	33 (32.7)
Negative	64 (63.4)
Unknown	4 (4.0)
PD-L1 in tumour cells, n (%)	
Positive	3 (3.0)
Negative	98 (97.0)
PD-L1 in tumour stroma, n (%)	
Positive	12 (11.9)
Negative	89 (88.1)
Immune cell score, n (%)	
Low	65 (64.4)
High	34 (35.6)
Stromal hyaluronan expression, n (%)	
Low	43 (42.6)
High	58 (57.4)
CD73 expression in tumour cells, n (%)	
Low	67 (66.3)
High	34 (33.7)

Table 1. Clinicopathological characteristics.

Dnro 10,832/06.01.03.01/2014). This study was designed and performed according to the reporting recommendations for tumour marker prognostic studies (REMARK) and the Declaration of Helsinki^{47,48}.

Results

Patient demographics. A total of 101 of PDAC patients were included in this study. The distribution of key clinicopathological variables among these patients is shown in Table 1.

Associations between stromal HA expression and other histopathological variables. Stromal HA accumulation appeared to associate with low ICS ($p=0.017$). The associations between stromal HA expression and other clinical and histopathological variables, cell-specific CD73 positivity and PD-L1 positivity in tumour cells were also assessed and are shown in Table 2. Stromal HA accumulation was not associated with

	HA high, n (%)	HA low, n (%)	p Value
Gender			
Male	33 (56.9)	20 (46.5)	0.301
Female	25 (43.1)	23 (53.5)	
T-stage			
pT1	2 (3.4)	1 (2.3)	0.742
pT2	14 (24.1)	8 (18.6)	
pT3	42 (72.4)	34 (79.1)	
pT4	0	0	
N-stage			
pN0	19 (32.8)	11 (25.6)	0.435
pN1	39 (67.2)	32 (74.4)	
Stage			
IA	2 (3.4)	1 (2.3)	0.979
IB	4 (6.9)	3 (7.0)	
IIA	12 (20.7)	8 (18.6)	
IIB	40 (69.0)	21 (72.1)	
Histological grade			
1	16 (30.2)	13 (30.2)	0.994
2	33 (62.3)	27 (62.8)	
3	4 (7.5)	3 (7.0)	
Perineural invasion			
Positive	35 (64.8)	29 (67.4)	0.786
Negative	19 (35.2)	14 (32.6)	
PD-L1 in tumour cells			
Positive	1 (1.7)	2 (4.7)	0.392
Negative	57 (98.3)	41 (95.3)	
PD-L1 in tumour stroma			
Positive	6 (10.3)	6 (14.0)	0.579
Negative	52 (89.7)	37 (86.0)	
Immune cell score			
Low	43 (74.1)	22 (51.2)	0.017
High	15 (25.9)	21 (48.8)	
CD73 in tumour cells			
Low	39 (67.2)	28 (65.1)	0.823
High	19 (32.8)	15 (34.9)	

Table 2. Clinicopathological variables and their association with stromal hyaluronan (HA).

other clinicopathological parameters, including CD73 positivity in tumour cells and PD-L1 positivity in tumour cells and stromal cells.

Stromal HA accumulation and survival. Regarding the whole study group, the median follow-up time was 44 (IQR 15.0 to 57.0) months for those alive at the end of follow-up. The estimated median OS for all patients was 25 months [95% CI: (17.7–32.3)]. Stromal HA accumulation was significantly associated with poor DSS ($p=0.037$) and OS ($p=0.013$) (Fig. 5).

In the multivariate analysis, stromal HA accumulation was an independent negative prognostic factor together with histopathological grade, TNM stage, CD73 positivity in tumour cells and low ICS (Table 3).

Discussion

In the present study, using a larger, consecutive patient series from a single geographical area of Northern Finland without apparent selection bias, we showed the role of stromal HA accumulation as an independent prognostic factor for poor survival in pancreatic cancer. We also found an association between the HA accumulation and low immune response as judged by the tumour-infiltrating T-cell densities.

While the number of patients in the present work was higher than in previous studies on HA in PDAC^{6,24}, an even larger material would probably have allowed a connection between T-cell score and hyaluronan stronger than that now established. The small tissue cores turned out to be quite acceptable for the analysis since in preliminary tests the HA intensities were strongly correlated between different cores of the same tumour even between the tumour centre and invasive margin. The computer-assisted evaluation of HA staining adopted for

	Univariate analysis (OS) ^a HR (95% CI)	<i>p</i>	Univariate analysis (DSS) ^b HR (95% CI)	<i>p</i>	Multivariate analysis (OS) HR (95%CI)	<i>p</i>	Multivariate analysis (DSS) HR (95% CI)	<i>p</i>
Stromal HA								
Low	1	0.015	1	0.042	1	0.019	1	0.048
High	1.80 (1.22–2.88)		1.67 (1.02–2.72)		1.85 (1.11–3.10)		1.71 (1.00–2.92)	
CD73 (TC)^c								
Negative	1	0.022	1	0.029	1	0.015	1	0.023
Positive	1.76 (1.09–2.84)		1.76 (1.06–2.93)		2.01 (1.14–3.53)		2.00 (1.10–3.62)	
Tumor grade								
1	1	0.006	1	0.013	1	0.012	1	0.019
2	1.95 (1.14–3.34)		1.95 (1.12–3.39)		1.99 (1.15–3.44)		2.01 (1.14–3.56)	
3	3.88 (1.54–9.79)		3.69 (1.36–10.01)		3.96 (1.36–11.52)		3.80 (1.18–12.01)	
TNM stage								
IA + IB	0.64 (0.28–1.48)	0.234	0.69 (0.30–1.61)	0.117	0.53 (0.21–1.36)	0.055	0.58 (0.22–1.52)	0.036
IIA	0.55 (0.29–1.06)		0.49 (0.24–0.99)		0.49 (0.25–0.95)		0.41 (0.20–0.85)	
IIB	1		1		1		1	
ICS^d								
High	1	0.007	1	0.008	1	0.006	1	0.002
Low	1.99 (1.21–3.30)		2.05 (1.21–3.47)		2.23 (1.26–3.95)		2.54 (1.40–4.63)	

Table 3. Multivariate analysis with Cox proportional hazard model. ^aOverall survival. ^bDisease specific survival. ^cTumour cell. ^dImmune cell score.

the present work was felt easier than manual scoring of sometimes minor differences in intensity. It can also be recommended for future studies due to its independence of personal variation between evaluators.

Stromal HA accumulation in malignancies originating from non-stratified epithelium is associated with a poor survival in a number of solid tumours⁷. Indeed, given the large desmoplastic stroma in PDAC, a major role of HA was expected in the progression of this cancer. The idea was further supported for example by a fact that a drug specifically reducing HA synthesis inhibits human PDAC cell growth in vitro and in mice in vivo⁴⁹. However, clinical trials combining enzymatic removal of HA and cytostatic drugs have been disappointing^{50,51} suggesting that it is not just the content of HA that enhances malignant growth. Rather, activated synthesis and concurrent degradation of HA probably provide an environment supporting cancer spreading⁷. This becomes understandable by considering the two opposite influences of HA on cell migration. By its swelling pressure HA gel creates free space for cells to move in, while at the same time blocks attachment to adjacent cells and matrix proteins.

Indeed, the cell surface hyaluronidase TMEM2 is an independent negative prognostic factor in PDAC⁵², demonstrating the importance of HA degradation in PDAC progression. TMEM2 associates to integrins and clears HA to facilitate cancer cell adhesion and migration⁵³. Besides facilitating migration in HA-rich matrix the fragments created by hyaluronidase act as a signal that amplify inflammation.

Increasing numbers of studies have shown the impact of HA on the host immune response: It is suggested to protect tumour cells against immune attack by forming peri-cellular coats⁵⁴. Moreover, HA accumulation seems to facilitate tumour-associated macrophage infiltration and their differentiation into the pro-tumoral M2 phenotype^{25,42} with an immunosuppressive effect preventing antitumour immunity by T-cells. Interestingly, in the present study we demonstrate an inverse correlation between T-cell-based ICS and stromal HA accumulation in PDAC. This supports the idea that an HA-rich extracellular matrix not only acts as a shield between T-cells and tumour cells, but also prevents T-cell infiltration in the whole tumour microenvironment. We have previously published a paper showing that CD73 positivity in PDAC cells is a prognostic factor in PDAC independently of ICS and hypothesized that CD73 suppresses immune response by impacting on the activity of the tumour infiltrating lymphocytes rather than their number³⁹. This might also explain why stromal HA expression associates with ICS but not with CD73 or PD-L1.

Recently, different phenotypes of ECM-producing cancer-associated fibroblasts (CAFs) have been described, including inflammatory CAFs and myofibroblastic CAFs⁵⁵. Inflammatory CAFs are supposed to be tumour-promoting via immune suppression⁵⁶. In future, it would be reasonable to find out if the HA accumulation associates with the polarization of CAFs, since this would further give some insight into the potential mechanism behind the association between HA and immune status. One possible link between CAF polarisation and HA synthesis is the STAT3-signaling pathway, since the inhibition of STAT3—pathway has been shown to downregulate HA—synthesis⁵⁷ and, on the other hand, to promote differentiation of CAFs into myCAFs⁵⁶.

As far as we know, the association of HA on T-cell immune response has not been studied earlier in PDAC but the present finding clearly warrants further expansion of the studies to obtain a more detailed view of the interactions between HA and lymphocytes in this disease with such a bleak prognosis. In future studies, information of physical properties (for example molecular mass) of HA molecules is also needed, since there are data indicating that molecular weight affects the biological functions of HA molecules⁵⁸.

In conclusion, our study indicates that stromal HA accumulation may be associated with low T cell densities in the PDAC microenvironment, but still represents an adverse prognostic parameter independent of T

cell densities, tumour stage, tumour grade, and CD73 expression. The results warrant further definition of the interactions between T-cell immunity and hyaluronan in the tumour microenvironment.

Received: 26 February 2021; Accepted: 26 May 2021

Published online: 09 June 2021

References

- Luo, J., Xiao, L., Wu, C., Zheng, Y. & Zhao, N. The incidence and survival rate of population-based pancreatic cancer patients: Shanghai Cancer Registry 2004–2009. *PLoS ONE* **8**(10), e76052 (2013).
- Ferlay, J. *et al.* Cancer incidence and mortality worldwide: Sources, methods and major patterns in GLOBOCAN 2012. *Int. J. Cancer* **136**(5), E359–E386 (2015).
- Ene-Obong, A. *et al.* Activated pancreatic stellate cells sequester CD8+ T cells to reduce their infiltration of the juxtatumoral compartment of pancreatic ductal adenocarcinoma. *Gastroenterology* **145**(5), 1121–1132 (2013).
- Hiraoka, N., Onozato, K., Kosuge, T. & Hirohashi, S. Prevalence of FOXP3+ regulatory T cells increases during the progression of pancreatic ductal adenocarcinoma and its premalignant lesions. *Clin. Cancer Res.* **12**(18), 5423–5434 (2006).
- Tammi, R. H. *et al.* Hyaluronan in human tumors: Pathobiological and prognostic messages from cell-associated and stromal hyaluronan. *Semin Cancer Biol.* **18**(4), 288–295 (2008).
- Whatcott, C. J. *et al.* Desmoplasia in primary tumors and metastatic lesions of pancreatic cancer. *Clin. Cancer Res.* **21**(15), 3561–3568 (2015).
- Tammi, M. I. *et al.* Activated hyaluronan metabolism in the tumor matrix—Causes and consequences. *Matrix Biol.* **78–79**, 147–164 (2019).
- Kuipers, H. F. *et al.* Hyaluronan synthesis is necessary for autoreactive T-cell trafficking, activation, and Th1 polarization. *Proc. Natl. Acad. Sci. U. S. A.* **113**(5), 1339–1344 (2016).
- Arufo, A., Stamenkovic, I., Melnick, M., Underhill, C. B. & Seed, B. CD44 is the principal cell surface receptor for hyaluronate. *Cell* **61**(7), 1303–1313 (1990).
- Turley, E. A. Hyaluronan and cell locomotion. *Cancer Metastasis Rev.* **11**(1), 21–30 (1992).
- Nikitovic, D., Tzardi, M., Berdiaki, A., Tsatsakis, A. & Tzanakakis, G. N. Cancer microenvironment and inflammation: Role of hyaluronan. *Front. Immunol.* **6**, 169 (2015).
- Porsch, H. *et al.* Efficient TGF β -induced epithelial-mesenchymal transition depends on hyaluronan synthase HAS2. *Oncogene* **32**(37), 4355–4365 (2013).
- Chanmee, T. *et al.* Hyaluronan production regulates metabolic and cancer stem-like properties of breast cancer cells via hexosamine biosynthetic pathway-coupled HIF-1 signaling. *J. Biol. Chem.* **291**(46), 24105–24120 (2016).
- Llaneza, A. *et al.* Hyaluronic acid as prognostic marker in resectable colorectal cancer. *Br. J. Surg.* **87**(12), 1690–1696 (2000).
- Theocharis, A. D., Vynios, D. H., Papageorgakopoulou, N., Skandalis, S. S. & Theocharis, D. A. Altered content composition and structure of glycosaminoglycans and proteoglycans in gastric carcinoma. *Int. J. Biochem. Cell Biol.* **35**(3), 376–390 (2003).
- García, I. *et al.* Relationship of tumoral hyaluronic acid and cathepsin D contents with histological type of gastric carcinoma. *Int. J. Biol. Markers* **15**(3), 215–218 (2000).
- Hopwood, J. J. & Dorfman, A. Glycosaminoglycan synthesis by Wilms' tumor. *Pediatr. Res.* **12**(1), 52–56 (1978).
- Roboz, J., Greaves, J., Silides, D., Chahinian, A. P. & Holland, J. F. Hyaluronic acid content of effusions as a diagnostic aid for malignant mesothelioma. *Cancer Res.* **45**(4), 1850–1854 (1985).
- Fukunaga, A. *et al.* CD8+ tumor-infiltrating lymphocytes together with CD4+ tumor-infiltrating lymphocytes and dendritic cells improve the prognosis of patients with pancreatic adenocarcinoma. *Pancreas* **28**(1), e26–31 (2004).
- Horai, T., Nakamura, N., Tateishi, R. & Hattori, S. Glycosaminoglycans in human lung cancer. *Cancer* **48**(9), 2016–2021 (1981).
- Takeuchi, J. *et al.* A high level of glycosaminoglycan-synthesis of squamous cell carcinoma of the parotid gland. *Cancer* **47**(8), 2030–2035 (1981).
- Kojima, J., Nakamura, N., Kanatani, M. & Omori, K. The glycosaminoglycans in human hepatic cancer. *Cancer Res.* **35**(3), 542–547 (1975).
- Lipponen, P. *et al.* High stromal hyaluronan level is associated with poor differentiation and metastasis in prostate cancer. *Eur. J. Cancer* **37**(7), 849–856 (2001).
- Cheng, X. B., Sato, N., Kohi, S. & Yamaguchi, K. Prognostic impact of hyaluronan and its regulators in pancreatic ductal adenocarcinoma. *PLoS ONE* **8**(11), e80765 (2013).
- Tiainen, S. *et al.* High numbers of macrophages, especially M2-like (CD163-positive), correlate with hyaluronan accumulation and poor outcome in breast cancer. *Histopathology* **66**(6), 873–883 (2015).
- Auvinen, P. *et al.* Hyaluronan in peritumoral stroma and malignant cells associates with breast cancer spreading and predicts survival. *Am. J. Pathol.* **156**(2), 529–536 (2000).
- Ropponen, K. *et al.* Tumor cell-associated hyaluronan as an unfavorable prognostic factor in colorectal cancer. *Cancer Res.* **58**(2), 342–347 (1998).
- Setälä, L. P. *et al.* Hyaluronan expression in gastric cancer cells is associated with local and nodal spread and reduced survival rate. *Br. J. Cancer* **79**(7–8), 1133–1138 (1999).
- Köbel, M. *et al.* Epithelial hyaluronic acid and CD44v6 are mutually involved in invasion of colorectal adenocarcinomas and linked to patient prognosis. *Virchows Arch.* **445**(5), 456–464 (2004).
- Anttila, M. A. *et al.* High levels of stromal hyaluronan predict poor disease outcome in epithelial ovarian cancer. *Cancer Res.* **60**(1), 150–155 (2000).
- Böhm, J. *et al.* Hyaluronan expression in differentiated thyroid carcinoma. *J. Pathol.* **196**(2), 180–185 (2002).
- Anitei, M. G. *et al.* Prognostic and predictive values of the immunoscore in patients with rectal cancer. *Clin. Cancer Res.* **20**(7), 1891–1899 (2014).
- Hatogai, K. *et al.* Comprehensive immunohistochemical analysis of tumor microenvironment immune status in esophageal squamous cell carcinoma. *Oncotarget* **7**(30), 47252–47264 (2016).
- Jiang, W. *et al.* Tumor-infiltrating immune cells and prognosis in gastric cancer: A systematic review and meta-analysis. *Oncotarget* **8**(37), 62312–62329 (2017).
- Wang, M. ImmunoScore predicts gastric cancer postsurgical outcome. *Lancet Oncol.* **18**(2), e68 (2017).
- Fridman, W. H., Pages, F., Sautès-Fridman, C. & Galon, J. The immune contexture in human tumours: Impact on clinical outcome. *Nat. Rev.* **12**(4), 298–306 (2012).
- Tahkola, K. *et al.* High immune cell score predicts improved survival in pancreatic cancer. *Virchows Arch.* **472**(4), 653–665 (2018).
- Zhuan-Sun, Y. *et al.* Prognostic value of PD-L1 overexpression for pancreatic cancer: Evidence from a meta-analysis. *Onco Targets Ther.* **10**, 5005–5012 (2017).
- Tahkola, K. *et al.* Prognostic impact of CD73 expression and its relationship to PD-L1 in patients with radically treated pancreatic cancer. *Virchows Arch.* **478**(2), 209–217 (2020).

40. Clark, A. G. & Vignjevic, D. M. Modes of cancer cell invasion and the role of the microenvironment. *Curr. Opin. Cell Biol.* **36**, 13–22 (2015).
41. Kim, R., Emi, M. & Tanabe, K. Cancer immunoeediting from immune surveillance to immune escape. *Immunology* **121**(1), 1–14 (2007).
42. Kuang, D.-M. *et al.* Tumor-derived hyaluronan induces formation of immunosuppressive macrophages through transient early activation of monocytes. *Blood* **110**(2), 587–595 (2007).
43. Iijima, J., Konno, K. & Itano, N. Inflammatory alterations of the extracellular matrix in the tumor microenvironment. *Cancers (Basel)* **3**(3), 3189–3205 (2011).
44. Edge, S. B. *et al.* (eds) *AJCC Cancer Staging Manual* (Springer, 2010).
45. Bosman, F. T. *et al.* (eds) *WHO Classification of Tumours of the Digestive System* (WHO, 2010).
46. Bankhead, P. *et al.* QuPath: Open source software for digital pathology image analysis. *Sci. Rep.* **7**(1), 16878 (2017).
47. World Medical Association. World Medical Association Declaration of Helsinki: Ethical principles for medical research involving human subjects. *JAMA* **310**(20), 2191–2194 (2013).
48. McShane, L. M. *et al.* REporting recommendations for tumour MARKer prognostic studies (REMARK). *Br. J. Cancer* **93**(4), 387–391 (2005).
49. Hajime, M. *et al.* Inhibitory effect of 4-methylesculetin on hyaluronan synthesis slows the development of human pancreatic cancer in vitro and in nude mice. *Int. J. Cancer* **120**(12), 2704–2709 (2007).
50. Ramanathan, R. K. *et al.* Phase IB/II randomized study of FOLFIRINOX plus pegylated recombinant human hyaluronidase versus FOLFIRINOX alone in patients with metastatic pancreatic adenocarcinoma: SWOG S1313. *J. Clin. Oncol. Off. J. Am. Soc. Clin. Oncol.* **37**(13), 1062–1069 (2019).
51. Van Cutsem, E. *et al.* Randomized phase III trial of pegvorhyaluronidase alfa with nab-paclitaxel plus gemcitabine for patients with hyaluronan-high metastatic pancreatic adenocarcinoma. *J. Clin. Oncol. Off. J. Am. Soc. Clin. Oncol.* **38**(27), 3185–3194 (2020).
52. Kudo, Y. *et al.* Overexpression of transmembrane protein 2 (TMEM2), a novel hyaluronidase, predicts poor prognosis in pancreatic ductal adenocarcinoma. *Pancreatol. Off. J. Int. Assoc. Pancreatol.* **20**(7), 1479–1485 (2020).
53. Irie, F. *et al.* The cell surface hyaluronidase TMEM2 regulates cell adhesion and migration via degradation of hyaluronan at focal adhesion sites. *J. Biol. Chem.* **296**, 100481 (2021).
54. Gately, C. L. *et al.* In vitro studies on the cell-mediated immune response to human brain tumors. II. Leukocyte-induced coats of glycosaminoglycan increase the resistance of glioma cells to cellular immune attack. *J. Immunol.* **133**(6), 3387–3395 (1984).
55. Öhlund, D. *et al.* Distinct populations of inflammatory fibroblasts and myofibroblasts in pancreatic cancer. *J. Exp. Med.* **214**(3), 579–596 (2017).
56. Biffi, G. *et al.* IL1-induced JAK/STAT signaling is antagonized by TGF β to shape CAF heterogeneity in pancreatic ductal adenocarcinoma. *Cancer Discov.* **9**(2), 282–301 (2019).
57. King, A. *et al.* Interleukin-10 regulates the fetal hyaluronan-rich extracellular matrix via a STAT3-dependent mechanism. *J. Surg. Res.* **184**(1), 671–677 (2013).
58. Jiang, D., Liang, J. & Noble, P. W. Hyaluronan as an immune regulator in human diseases. *Physiol. Rev.* **91**(1), 221–264 (2011).

Acknowledgements

We thank Eija Rahunen for her excellent assistance in HA stainings.

Author contributions

All authors met the criteria listed in the ICMJE recommendations for the qualification of authorship. K.T. and J.B. had full access to all the data and take responsibility for the integrity of the data and the accuracy of the analysis. Concept and design: K.T., J.M. and J.B. Acquisition, analysis, or interpretation of data: All authors. Drafting of the manuscript: K.T., J.V. and J.B. Critical revision of the manuscript for important intellectual content: All authors. Statistical analysis: K.T. and J.B. Administrative, technical, or material support: All authors. Supervision: J.M., J.L., I.K. and J.B.

Funding

This study received funding from the Cancer Foundation Finland, the Finnish Medical Foundation, the Jane and Aatos Erkko Foundation, the Emil Aaltonen Foundation and the State Research Funding.

Competing interests

The authors declare no competing interests.

Additional information

Supplementary Information The online version contains supplementary material available at <https://doi.org/10.1038/s41598-021-91796-x>.

Correspondence and requests for materials should be addressed to K.T.

Reprints and permissions information is available at www.nature.com/reprints.

Publisher's note Springer Nature remains neutral with regard to jurisdictional claims in published maps and institutional affiliations.



Open Access This article is licensed under a Creative Commons Attribution 4.0 International License, which permits use, sharing, adaptation, distribution and reproduction in any medium or format, as long as you give appropriate credit to the original author(s) and the source, provide a link to the Creative Commons licence, and indicate if changes were made. The images or other third party material in this article are included in the article's Creative Commons licence, unless indicated otherwise in a credit line to the material. If material is not included in the article's Creative Commons licence and your intended use is not permitted by statutory regulation or exceeds the permitted use, you will need to obtain permission directly from the copyright holder. To view a copy of this licence, visit <http://creativecommons.org/licenses/by/4.0/>.

© The Author(s) 2021